4-22-2022

Three-Heartbeat Multilead ECG Recognition Method for Arrhythmia Classification

Liang-Hung Wang

Yan-Ting Yu

Wei Liu

Lu Xu

Chao-Xin Xie

See next page for additional authors

Authors

Liang-Hung Wang, Yan-Ting Yu, Wei Liu, Lu Xu, Chao-Xin Xie, Tao Yang, I-Chun Kuo, Xin-Kang Wang, Jie Gao, and Patricia Angela R. Abu

IEEE Access
Multidisciplinary | Rapid Review | Open Access Journal

Received April 1, 2022, accepted April 16, 2022, date of publication April 22, 2022, date of current version April 29, 2022.

Digital Object Identifier 10.1109/ACCESS.2022.3169893

Three-Heartbeat Multilead ECG Recognition Method for Arrhythmia Classification

LIANG-HUNG WANG[1], (Senior Member, IEEE), YAN-TING YU[1], WEI LIU[1], LU XU[1], CHAO-XIN XIE[1], TAO YANG[1], I-CHUN KUO[2], XIN-KANG WANG[3], JIE GAO[3], PAO-CHENG HUANG[4], SHIH-LUN CHEN[5], (Member, IEEE), WEI-YUAN CHIANG[6], AND PATRICIA ANGELA R. ABU[7], (Member, IEEE)

[1]Department of Microelectronics, College of Physics and Information Engineering, Fuzhou University, Fuzhou 350108, China
[2]College of Biological Science and Engineering, Fuzhou University, Fuzhou 350108, China
[3]Department of Electrocardiogram, Fujian Provincial Hospital, Fuzhou 350001, China
[4]College of Computer and Information Sciences, Fujian Agriculture and Forestry University, Fuzhou 350002, China
[5]Department of Electronic Engineering, Chung Yuan Christian University, Taoyuan City 320314, Taiwan
[6]National Synchrotron Radiation Research Center, Hsinchu 30076, Taiwan
[7]Department of Information Systems and Computer Science, Ateneo de Manila University, Quezon City 1108, Philippines

Corresponding author: Liang-Hung Wang (eetommy@fzu.edu.cn)

This work was supported in part by the National Natural Science Foundation of China under Grant 61971140, in part by the Major Project of Ministry of Science and Technology under Grant 2020IM010200, in part by the Major Project and Innovation Platform of Science and Technology Agency of Fujian Province under Grant 2021H6003, and in part by the Health and Education Project of Fujian Province under Grant 2021D036 and Grant 2019-WJ-18.

ABSTRACT Electrocardiogram (ECG) is the primary basis for the diagnosis of cardiovascular diseases. However, the amount of ECG data of patients makes manual interpretation time-consuming and onerous. Therefore, the intelligent ECG recognition technology is an important means to decrease the shortage of medical resources. This study proposes a novel classification method for arrhythmia that uses for the very first time a three-heartbeat multi-lead (THML) ECG data in which each fragment contains three complete heartbeat processes of multiple ECG leads. The THML ECG data pre-processing method is formulated which makes use of the MIT-BIH arrhythmia database as training samples. Four arrhythmia classification models are constructed based on one-dimensional convolutional neural network (1D-CNN) combined with a priority model integrated voting method to optimize the integrated classification effect. The experiments followed the recommended inter-patient scheme of the Association for the Advancement of Medical Instrumentation (AAMI) recommendations, and the practicability and effectiveness of THML ECG data are proved with ablation experiments. Results show that the average accuracy of the N, V, S, F, and Q classes is 94.82%, 98.10%, 97.28%, 98.70%, and 99.97%, respectively, with the positive predictive value of the N, V, S, and F classes being 97.0%, 90.5%, 71.9%, and 80.4%, respectively. Compared with current studies, the THML ECG data can effectively improve the morphological integrity and time continuity of ECG information and the 1D-CNN model of ECG sequence has a higher accuracy for arrhythmia classification. The proposed method alleviates the problem of insufficient samples, meets the needs of medical ECG interpretation and contributes to the intelligent dynamic research of cardiac disease.

INDEX TERMS Arrhythmia classification, electrocardiogram, one-dimensional convolutional neural network (1D-CNN), priority model integrated voting method, three-heartbeat multi-lead (THML).

I. INTRODUCTION

Electrocardiogram (ECG) is a non-invasive diagnostic tool of pathological information about heart conditions and plays an important role in the classification of cardiovascular diseases (CVDs). CVD is one of the chronic aging diseases and is a leading cause of death, especially in the elderly [1]–[4]. Globally, the aging population is a major driver of this trend in cardiovascular mortality. By 2030, almost 23.6 million people are expected to die from CVDs, mainly from heart disease and stroke [5]. According to the World Health Organization, as of 2020, CVDs are still the number one

The associate editor coordinating the review of this manuscript and approving it for publication was Vishal Srivastava.

cause of death globally [6]. The global cardiovascular problems are becoming increasingly serious with the aging of the population and other factors. A routine procedure for diagnosing CVD is to take an electrocardiogram of patients and determine the type of disease through an interpretation from experienced physician. However, this approach increases the burden the work of doctors. Therefore, computer-aided diagnosis technology needs to be introduced to alleviate the shortage of resources for CVD treatment and diagnosis.

Traditional machine learning algorithms depend on manual selection of features [7]–[12], and different studies use different features, such as R-R interval, Q-T interval, P-R interval, wavelet features, independent component analysis morphological feature, and nonlinear features [13]–[18]. Tang *et al.* [17] proposed linear-kernel support vector machine (SVM) classifier, which combines global and local classifiers to classify arrhythmia. Acharya *et al.* [18] designed automated classification using K-nearest neighbor and decision tree classifiers in arrhythmia diagnosis. Ince *et al.* [19] adopted artificial neural network to solve significant inter-patient variations. Machine learning classifiers have a limited ability to classify arrhythmias by extracting features [17]–[21]. These features have difficulty fully describing the disease, because the process of extracting features will omit waveform detail information or add the redundancy of features.

Compared with traditional machine learning, deep learning can extract features more comprehensively and scientifically, and achieve end-to-end learning. A convolutional neural network (CNN), as a typical method in deep learning, plays an important role in image processing. CNN can be applied not only in the field of two-dimensional images but also in the field of one-dimensional data, such as natural language processing [22] and some physiological signals (such as blood pressure signal [23], respiratory signal [24], [25], and ECG signal [26]–[31]. In terms of characteristics of the ECG signal, the ECG classification can be divided into two cases, namely, single-heartbeat ECG [27], [28], and fixed-length ECG [29]–[31]. Kandala *et al.* employed an adaptive non-stationary and nonlinear decomposition method, namely ICEEMD, to analyze each ECG heartbeats which contains 300 sampling points. Although the method improves the classification effect of N and V classes, the effect of rare arrhythmia types is not ideal. Shi *et al.* [28] studied on weighted extreme gradient boosting (XGBoost) to reduce the impact of imbalance in the dataset, and proposed a hierarchical classification method of single heartbeat ECG sample. The classification performance of abnormal heart rhythm has been improved, but the problem of insufficient sample data has not been solved. Yang *et al.* [29] proposes a 12-lead ECG arrhythmia classification method using a cascaded convolutional neural network and multiple ECG leads, while the network computing burden is heavy. Acharya *et al.* [31] implemented data pre-processing by intercepting a fixed ECG length of two or five seconds and assigning a label to each segment. In this way, the number of heartbeats in each sample is not fixed and may contain incomplete heartbeat waveforms, which cannot be well classified and applied to clinical diagnosis.

In summary, the corresponding challenges that still exist in the field of intelligent ECG classification mainly include the following points. Traditionally, the sample segmentation of ECG data by fixed-length, and the information of the sample may be incomplete or redundant, which is not conducive to the realization of intelligent network learning. Moreover, some ECG samples of patient that can be used for deep learning are insufficient, which is not conducive to the development of ECG automatic classification. In addition, with the rapid development of portable ECG device, a large number of long-term ECG activity from patients can be recorded. To convert the collected ECG sequence data from portable device into image data do not only increases the time cost, but also requires a large amount of storage resources and computing costs. Therefore, the development of neural network architecture suitable for ECG sequence signals can provide technical support for ECG recognition on portable devices. Therefore, we propose to use three-heartbeat multi-lead (THML) ECG data, in which each fragment contains three complete heartbeat processes of multiple ECG leads. The THML ECG data not only enables the transformation from single-heartbeat classification to multi-heartbeat classification, but also contains a large number of important related ECG waveform features of anterior and posterior heartbeats. Correspondingly, this study proposes the arrhythmia classification method of THML ECG data based on one-dimensional convolutional neural network (1D-CNN) and MIT-BIH arrhythmia database. The proposed classification method is divided into three parts:

1) Complete pre-processing scheme for the characteristics of THML ECG data, which innovatively cut and define the label of each THML ECG data.
2) Construction of four 1D-CNN models with different hyperparameters for different types of arrhythmias. Compared with previous papers, the accuracy of the four models using THML ECG data as input can reach about 90% if the training and test samples are completely independent and not crossed according to the Association for the Advancement of Medical Instrumentation (AAMI) standard.
3) A priority model integrated voting method was proposed to achieve the optimal solutions and further improve the accuracy by integrating the four models. The final average accuracy of five categories of arrhythmia is above 94%.

The results based on the MIT-BIH arrhythmia benchmark database demonstrate that the proposed inter-patient arrhythmia classification system with THML ECG data as input achieves superior performance over most classification methods that use single-heartbeat or fixed length ECG data. The experiment results also demonstrate that the 1D-CNN

TABLE 1. Mapping the MIT-BIH arrhythmia database heartbeat types to the AAMI heartbeat class.

Annotated Codes	Arrhythmia Beat type annotated in MIT-BIH	Corresponding arrhythmia class in AAMI
1	N (Normal beat)	N
2	L (Left bundle branch block beat)	
3	R (Right bundle branch block beat)	
11	j (Nodal (junctional) escape beat)	
34	e (Atrial escape beat)	
4	a (Aberrated atrial premature beat)	S
7	J (Nodal [junctional] premature beat)	
8	A (Atrial premature beat)	
9	S (Premature or ectopic supraventricular beat)	
5	V (Premature ventricular)	V
10	E (Ventricular escape beat)	
6	F (Fusion of ventricular and normal beat)	F
12	Paced beat	Q
13	Unclassifiable beat	
38	Fusion of paced and normal beat	

architecture can realize inter-patient arrhythmia classification with high performance.

The remainder of this paper is organized as follows: Section II introduces the MIT-BIH arrhythmia database and the pre-processing methods of THML ECG signals. Section III presents the architecture of inter-patient ECG arrhythmia classification model and the design of neural network. Section IV provides the performance evaluation results of the experiments. Section V discusses the corresponding comparison with other published literature and Section VI concludes this paper.

II. THREE-HEARTBEAT MULTI-LEAD ECG DATA PRE-PROCESSING

Most of the current arrhythmia studies are based on the classification of single-heartbeat and single-lead ECG data. As a result, the information about anterior and posterior heartbeats is excluded from the input data. In this study, we propose a method to classify arrhythmia based on THML ECG data and verify its feasibility in experiments. The ECG data in MIT-BIH arrhythmia database is pre-processed into THML ECG data. The pre-processing method consists of three parts: THML ECG data cutting, THML data relabeling, and signal resampling and filtering. To compare the training results of the THML ECG data with those of the fixed-length multi-heartbeat ECG data, we performed fixed-length ECG data processing as well.

A. DATASET

In this study, ECG datasets from the MIT-BIH arrhythmia database are used for the performance evaluation of the proposed inter-patient arrhythmia classification approach. This benchmark database contains 48 records of 47 individual subjects, each containing dual-channel ECG signals for a 30-minute duration, in which records 201 and 202 were from the same subject. Most records contain two ECG leads: lead II and lead V1. This database is recommended by the AAMI [32], and it includes the five essential arrhythmia group labels—N, V, F, S, and Q—as described in Table 1. In Table 1, the number of first column are the annotated codes for categories in the MIT-BIH database. The second column is the arrhythmia beat types annotated by MIT-BIH database. The third column is the arrhythmia types existing in MIT-BIH database mapped into corresponding AAMI heartbeat class.

We considered the inter-patient paradigm to evaluate the proposed classification method. In the inter-patient paradigm, the training and testing sets are constructed from different patients, following the protocol proposed by Chazal *et al.* [33]. In this method, the ECG data from the MIT-BIH database (44 records based on AAMI standard) are divided into two sets of records: DS1 = {101, 106, 108, 109, 112, 114, 115, 116, 118, 119, 122, 124, 201, 203, 205, 207, 208, 209, 215, 220, 223,230} and DS2 = {100, 103, 105, 111, 113, 117, 121, 123, 200, 202, 210, 212, 213, 214, 219, 221, 222, 228, 231, 232, 233, 234}. DS1 is used as a training set to build the classification model, and DS2 is utilized as a testing set to evaluate the model. This division approach guarantees that the records of patients are independent in both training and testing sets.

B. THML ECG DATA CUTTING AND RELABELING

Presently, the resting ECG commonly used in hospitals records the continuous cardiac electrical activity of patients in a short period, which can be used to diagnose arrhythmia, ventricular hypertrophy, and even determine the location of myocardial ischemia and myocardial infarction. In traditional ECG classification that uses samples cut which have some disadvantages. First, most of the related studies used single-lead ECG data and the fixed-length ECG segment, which would lead to incomplete ECG information. Clinically, single-heartbeat or fixed-length ECG data has its limitations and the data is not enough to provide a reference for diagnosis, thus, multi-heartbeat samples can better meet the needs of medical ECG intelligent interpretation [34]. Second, if the sampled length is too long, this may cause data redundancy and network computing burden may be caused. Therefore, the length of multi-heartbeat segments should be selected appropriately. Finally, the 12-lead ECG of patients reflects the physiological functions of different heart structures which is beneficial to the identification of abnormal heart rhythms or the diagnosis of heart diseases compared to single-lead ECG. Meanwhile, the use of multi-lead ECG can effectively solve the problem of shortage

TABLE 2. Statistics on the number of THML ECG data.

THML category	Raw label of THML segments	Number of raw label in DS1	Total number of THML in DS1	Number of raw label in DS2	Total number of THML in DS2
N	NNN	39791	39791	36167	36167
S	SSS	378	1581	866	2448
	SSN/NSS/SNS	153		836	
	SNN/NSN/NNS	1050		746	
V	VVV	369	7187	13	6646
	VVN/NVV/VNV	1890		1064	
	VNN/NNV/NVN	4928		5569	
F	FFF	0	377	0	721
	FNN/NFN/NNF	367		522	
	FFN/NFF/FNF	10		199	
Q	QQQ	1	20	0	12
	QNN/NQN/NNF	17		12	
	QQN/NQQ/QNQ	2		0	
Others	Two or more categories	949	949	212	212

The DS1 set is used as the training set, and the DS2 set is used as the testing set.

of clinical data. Considering the above factors, this study proposes the THML ECG segment to be used as the input samples, which contain a large number of important ECG data features, in comparison with single-lead single-heartbeat ECG data experiment, which has shown to have achieved a better effect.

The specific scheme for the cutting of THML data is as follows. First, Accurate location of R wave detection is a necessary condition for ECG signal analysis. In this study, the R-wave position provided in the MIT-BIH database is directly used, because the labeling file of MIT-BIH arrhythmia database provides the precise labeling of R-wave location. Second, the ECG signals from MIT-BIH database are cut into THML data. The traditional length-fixed cutting method can easily destroy the important wave position of the next ECG signal because the heartbeat rhythm of the patient can vary inconsistently. The approach proposed in this study innovatively slices ECG signals into THML ECG data that retains the complete morphological characteristics of ECG signals. As shown in Figure 1, a segment of raw ECG data exists, and the R-wave position is assumed to be {R0, R1, R2, R3, R4}. Every slice starts from the midpoint (M0) between the first R-wave position (R1) and the previous R-wave position (R0) and ends at the midpoint (M1) between the third R-wave position (R3) and the next R-wave position (R4). The THML ECG segment is {R1, R2, R3}. This approach ensures that each THML ECG segment contains three complete P-QRS-T waveforms. Finally, because the label of the MIT-BIH database is calibrated on a single heartbeat, problems using multiple label will occur when intercepting the THML data. In accordance with the AAMI standard classification rules, the following are used to formulate the THML data labels:

1) When all arrhythmia types of heartbeat in the THML ECG segment are N, the label of the segment is set as N class.
2) When two or more arrhythmia types except N class exist in the THML ECG segment, it will be deleted and will not be included for training.
3) When only one arrhythmia type except for N class exists in the THML ECG segment, the segment is labeled as the category that excludes N class (i.e., the original label of data is NFF, so the final label of THML data is F. If the original label is NNF, then the final label of THML data is also F. The order of each arrhythmia type is not considered).

Dropping the first R-wave of each record ensures that the method can be more accurate for the relabeling of THML ECG data. After adopting the above approach, we obtained the amount of various THML ECG data as listed, in Table 2.

C. THML DATA RESAMPLING AND FILTERING

Resampling refers to the process of converting a time series data from one frequency to another. Due to the difference in the heart rate of patients, the data length of each segment is unequal in the process of THML ECG data cut. But the input data of the CNN needs to be in uniform length; thus, the THML ECG data with different lengths need to be resampled into having a uniform length. Taking into account the average heart rate, the data sampling rate of the MIT-BIH database and the unified input format of convolutional network, this study resampled the THML ECG data to 1280 sampling points. The multiphase filter can be used to resample the data into a uniform length, and it provides a framework to solve the data sampling rate problem. The output rate of the signal is changed by interpolation, and the Nyquist sampling theorem is used to ensure that no aliasing occurs.

After THML ECG data filtering, zero-mean normalization (Z-score) method is adopted, which applies the mean value, standard deviation, and observed value of the overall data to achieve standardization by transforming the original data from different magnitude into uniform magnitude.

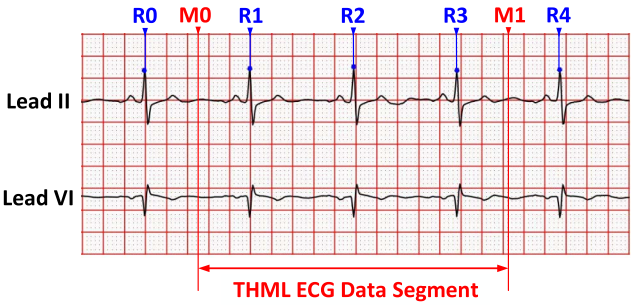

FIGURE 1. Schematic of the intercept of THML ECG data.

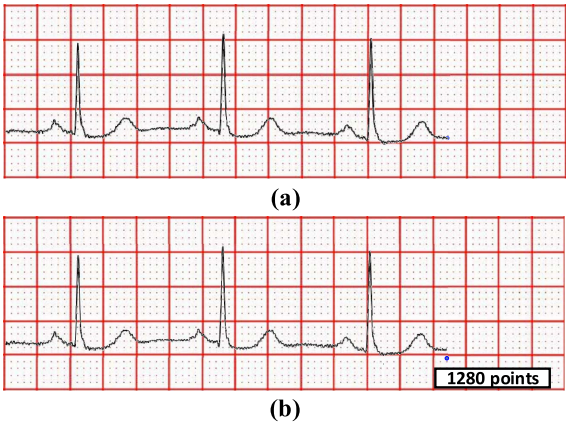

FIGURE 2. Before and after resampling contrast chart. (a) original three-heartbeat ECG data with the length of 961 fixed points before resampling. (b) three-heartbeat ECG data with the length of 1280 fixed points after resampling.

The resampled THML ECG data are clustered near 0 and presented a normal distribution after Z-score processing. The results before and after resampling of three-heartbeat ECG data are shown in Figure 2, where the number marked at the end of waveform represents the length of data point. This resampling process increases the number of data points from the original 961 sampling points to 1280 sampling points. At the same time, this improves the waveform which has no deformation stretch. Hence, resampling can effectively achieve a uniform data length.

As for filtering, this study adopted the wavelet de-noising method. It is known that the ECG signal energy is mainly concentrated in the range of 0.5Hz to 45Hz. Based on the wavelet basis function db6, the ECG signal of MIT-BIH database is de-noised based on a one-dimensional discrete wavelet transform through Equation (1). The ECG signal sampled at 360Hz is decomposed into 9 levels by db6 wavelet, and finally, the de-noised ECG signal is obtained.

D. THML ECG DATA BALANCE

As shown in Table 2, a significant imbalance exists in the THML ECG dataset. Compared with the largest number of N class, the number of Q, S, V, and F classes is significantly lesser. Under this condition, the THML ECG dataset is not conducive to network training and learning. This study proposes an approach to balance the data volume of each

TABLE 3. Statistics on the number of fixed-length ECG data.

Fixed-length ECG data category					
	N	S	V	F	Q
Total number in DS1	10478	408	2236	94	6
Total number in DS2	10361	696	2000	160	5

arrhythmia class. First, the number of cycles is calculated to determine the overlap length of the anterior and posterior points in each THML ECG segment and obtain the number of points needed to move in each cycle for small sample classes. The calculation formula is as follows:

$$k = floor\left(\frac{pl}{floor(K/x)}\right) \tag{1}$$

where k is the number of moving points, pl is the range of points that can be moved, x is the number of samples of the current category, K is the sample number of the largest category, and function "*floor*" means round down. Second, on the premise of not changing the main waveform characteristics of THML ECG data, new samples are obtained by moving k points. The THML ECG data of the DS1 training set is balance and not the data of test set DS2 because of the need for model training. The V, S, F, and Q classes of THML ECG data in DS1 were balanced using the above method and the balanced set is called Set A. The number of the various categories in Set A is N: 39791, V: 39525, S: 35940, F: 39585, and Q: 39780.

E. FIXED-LENGTH MULTI-HEARTBEAT ECG DATA

To compare the training results of the THML ECG data with those of the fixed-length ECG data, fixed-length ECG data processing is performed. The normal heartbeat rate is from 60 to 100 times/min, and the sampling rate of MIT-BIH data is 360 Hz/s. To make the fixed length of each sample close to the length of the three heartbeats, the fixed-length points for slicing is set to 1080 and no overlapping segments exist. The labels of the fixed-length ECG data are formulated by the rules of part B. The resulting amount of various fixed-length ECG data obtained are listed in Table 3.

The imbalance of fixed-length sample data also exists, and the way to alleviate the category imbalance is to equalize the number of samples in each category by overlapping the fragments. The N class with the largest sample size is considered as the benchmark to calculate the overlap length for cutting. The formula used to calculate for the overlap length is as follows:

$$ol = round\left(K_1\left(1 - \frac{K}{x}\right)\right) \tag{2}$$

where ol represents the overlapping length to be calculated; K_1 represents the fixed-length of each segment, which is

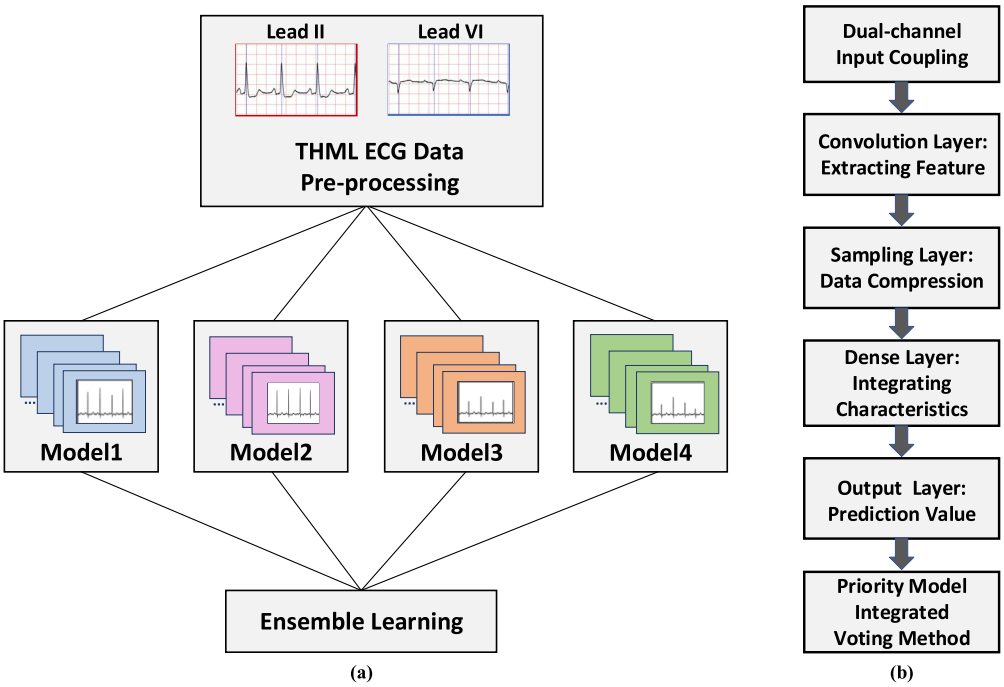

FIGURE 3. Framework of three-heartbeat multi-lead (THML) ECG recognition method. (a) system diagram of arrhythmia classification method. (b) function of each part in the system diagram.

1080; K represents the number of the largest sample size; and x represents the number of samples in the current category.

The number of the fixed-length ECG data of the training set DS1 is balance as needed for model training and this balanced fixed-length ECG data of DS1is called Set B. This method is the current mainstream, but accurately distinguishing the classification type of segment is difficult due to information loss. The number of each category in Set B is N: 10478, V: 10555, S: 10573, F: 10155, and Q: 5012. At this point, the pre-processing of the THML ECG dataset and the fixed-length ECG dataset has been completed.

III. ARRHYTHMIA CLASSIFICATION METHOD

In this study, the rationale of arrhythmia classification is as follows. The dual-lead ECG data in MIT-BIH arrhythmia database is pre-processed into THML ECG data and input into dual-channel 1D-CNN. Through the network, the subtle features in ECG signals that are difficult to find manually are extracted and analyzed. Four classification models were set for different arrhythmia types, and the priority model integrated voting method was used to optimize the classification results of the four models and thus improving the final classification effect of the system.

A. FRAMEWORK

The framework of the THML method for arrhythmia classification is shown in Figure 3. On the basis of the deep learning framework with TensorFlow platform as the back end, this study designs a dual-channel coupled network model based on 1D-CNN network to adapt to the dual-lead ECG data of MIT-BIH arrhythmia database. In the pre-processing stage, the ECG records from the MIT-BIH arrhythmia database are denoised, sliced into THML ECG data, and resampled into uniform length. After the pre-processing, the modified ECG lead II signals of the MIT-BIH database are taken as the first input channel, and the ECG lead V1 signals of the MIT-BIH database are taken as the second input channel. By introducing multiple lead features with the addition of channels, the network increases the information amount of the sample input data and improves the classification effect.

In this study, four 1D-CNN models were set up according to the different arrhythmia types. Through a comparison of the classification characteristics of different models, a priority model integrated voting method was proposed to integrate and optimize the classification effects of the four 1D-CNN models. The results of model ensemble learning are improved compared with each single model, and the feasibility of the optimization scheme is verified.

B. MULTI-LEAD COUPLING

Clinical ECG practices commonly use multi-lead ECG signals, and the characteristics of different ECG leads can facilitate the final classification results from different dimensions. If the classification is implemented by single ECG lead, then it is not comprehensive enough and easily misses the key features of many categories. However, most multi-lead ECG methods ignore the interrelation of each lead in the independent coding process. This study proposes a novel multi-lead coupling method based on the image multi-channel principle to classify THML ECG data.

The concept of channel originally refers to the channel of three primary colors (i.e., red, green, and blue) in the electronic picture. With the use of the multi-channel approach of images, the multi-lead ECG signal can be input as multiple channels, and the waveform from the multi-channel ECG can be superimposed into the tensor. Through multi-lead ECG data coupling, multilayer convolutions extract the correlation of multidimensional features.

This study uses the THML ECG data as dual-channel input to extract features, which contains modified lead II signal and lead V1 signal from the MIT-BIH arrhythmia database.

The convolution calculation process of the 1D-CNN network with dual-channel input is as follows:

(1) The input matrix format has three dimensions: sample size, data length, and channel number. Unlike the two-dimensional image input, the ECG signals do not need the input length and input width, only the input data length.

(2) The length of the output matrix is determined by the input matrix, convolution kernel, and scanning mode. The output matrix format is the same as the input matrix format by changing the size of the scanning mode and the size of the padding point. The formula used is as follows:

$$length_{out} = \frac{(length_{in} - length_{kernel} + 2 \times padding)}{stride} + 1 \quad (3)$$

where $length_{in}$, $length_{out}$, and $length_{kernel}$ represent the length of input data, the length of output data, and the length of convolution kernel, respectively. *Stride* and *padding* represent the step size and the complement point, respectively.

(3) The weight matrix (convolution kernel) format has three dimensions, which are the convolution kernel length, number of input channels, and number of output channels. The number of input channels in each layer is determined by the number of output channels in the last layer.

C. DUAL-CHANNEL 1D-CNN WITH RESIDUAL BLOCK

The 1D-CNN network is an effective way to obtain features that come from a shorter fixed-length fragment through the overall dataset [22]. This network is well applied to the time series analysis of sensor data and to the analysis processing of ECG data. ECG signals can take the form of one-dimensional sequences, instead of using the form of two-dimensional electrocardiogram, thus reducing a significant amount of redundant data.

The convolution operation process is as follows:

$$y(c) = \omega(c) * x(c) = \sum_{i=0}^{N} \omega\ (c-i)x(i) \quad (4)$$

where ω represents the convolution kernel, x represents the input signal, and y is the output of the convolution result. We regard the one-dimensional convolution kernel as a feature extractor.

As shown in Figure 4, the network architecture flowchart is divided into several parts, namely, the dual-channel input layer, pre-activation block, pre-residual block, residual block, post-residual block, and the output layer.

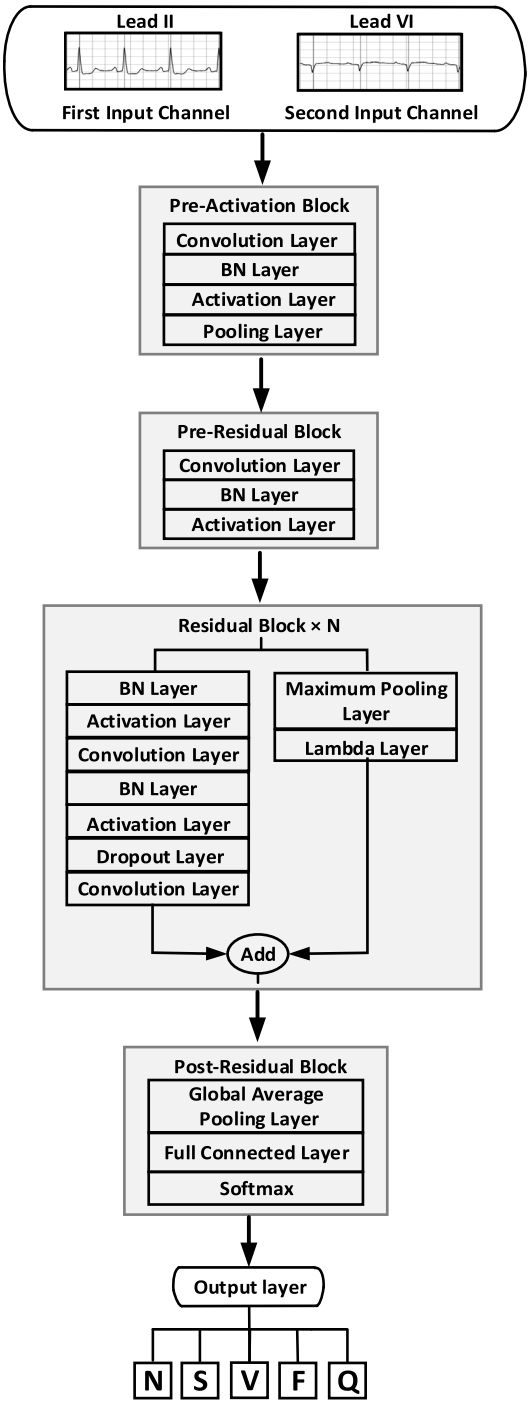

FIGURE 4. Network architecture flowchart.

The dual-channel input matrix of the network has two sequences (one from modified lead II, the other from lead V1) with a length of 1280 sampling points. In the pre-activation block, it ensures that the length of the output tensor remains unchanged after the convolution operation by setting the length of padding, and the number of output channels is the number of input convolution cores.

The residual network is introduced in the process of design to overcome network degradation due to network depth by

using identity mapping. The selection of important parameters and the design of some layers are improved according to the characteristics of THML ECG signals. Residual network is a cross-layer superposition process, which can easily lead to the mismatching of channel numbers between different layers and cannot be directly stacked. Therefore, a custom layer named lambda is added to the network, and the lambda layer fills the extra channels by padding it with zeros to match the number of anteroposterior channels. In the residual block shown in Figure 4, N represents the number of repetitions of the combined structure, and the multiple superposition structure plays an important role in the overall network. The network increases the number of convolution kernels to increase the number of channels. Then, the convolution layer reduces the feature length according to the step size and finally reaches the fully connected layer. The fully connected layer passes through the activation layer, where the activation function is the softmax function. Finally, N, V, S, F, and Q classes of the output are obtained, as illustrated in Figure 4.

In this study, an ECG signal is considered as a one-dimensional sequence which is different from the two-dimensional image signal. A small convolutional kernel with a size of 3×3 is commonly used in convolutional networks image classification. However, the ECG signal has a low frequency and low sampling rate, which makes it difficult to form a waveform with pathological feature significance at every three sampling points and is extremely vulnerable to high-frequency noise. Small convolution kernels pay too much attention to the disturbance caused by high-frequency noise and ignore the overall variation of the ECG signal. Using a slightly larger convolutional kernel can effectively alleviate this problem. The proposed network uses a larger one-dimensional convolution kernel, and the selection of the convolution kernel length has also been tested several times, including 16, 32, and other lengths. The number of convolution kernels is set to multiples of 12 and 16. According to the different settings of convolution kernel and network depth, four models are designed, namely, Model1, Model2, Model3, and Model4 where each model focuses on different arrhythmia types.

The parameters of the four models are listed in Table 4. The parameters of each convolutional layer are the convolution kernel size, number of convolution kernels, and stride length of sequence. With Model1 taken as an example, the convolution kernel size of Model1 is set to 32*1, which extracts the features between every 32 points. The number of convolution kernels in convolutional layer 1 to layer 5 is initially set to 12. The step size in convolutional layer 1 to 5 is set in sequence according to the stride = [1, 1, 1, 2, 1]. The remaining parameters of Model1 in other layers are listed in Table 4. Meanwhile, the method of supplementary points was adopted to keep the length of input and output data consistent. Finally, the convolution output size of the 17^{th} layer is 80×96, and the output size of the global average pooling layer is 1×96. After the softmax activation function, the final output is five categories of classification results.

From Table 4, we can see that the Model2 adds 8 convolutional layers compared with Model1, and extracts further features by increasing the depth of convolution. The convolution kernel size of Model3 is set to 32*1 in the first 12 convolutional layers and 16*1 in the last 6 convolutional layers. The two types of convolution kernels are used to extract features of different ranges, and the rest is consistent with Model1. The convolution kernel size of Model4 is set to 16*1, and then the number of convolution kernels is adjusted according to the step size.

Overfitting is an inevitable problem in the training process. In this study, many methods are adopted to solve overfitting problems and obtain good results. First, the dataset is amplified by using the method described in part C of Section II, which increases the sample size in general and balances the data amount of each category. Second, the L2 regularization is added to the weight of each layer to reduce the parameters in the training process and simplify the network. The L2 regularization can solve the overfitting problem by adding weight to the loss function and limiting the weight from increasing during the training process. Third, the dropout layer is added to the network design process and improves network generalization capability. The discard probability of dropout layer is set to 0.5.

The network optimizer adopts stochastic gradient descent and momentum optimization algorithm. The momentum coefficient is set as 0.9, and the learning rate α is set as a step descent mode. The downregulation changes of α happen through the iterative period, and the initial value is set as 0.1. The number of parameters in the designed 18-layer convolutional network is about 1.3 million, and the parameters of the designed 26-layer convolutional network are about 19.59 million.

Four ECG classification models were built during the experiments, and convolution parameters suitable for low frequency and low sampling rate characteristics of ECG were obtained which provided a reference for further study on one-dimensional ECG sequence correlation.

D. PRIORITY MODEL INTEGRATED VOTING METHOD

Ensemble learning is an effective technique to improve accuracy in various machine learning tasks. This study proposes a priority model integrated voting method that combines the majority voting method with the weighted voting method. The integration model was applied by setting priority weight and voting, and the classification effects of each model on different arrhythmia types were analyzed to improve the final prediction results.

The majority voting method aims to find the mode of the results of multiple classification models. For example, the classification results of the four models are assumed to be [N, N, V, S], and then the final voting judgment result is N class. If different categories have the same votes, then a random category with the same number is selected as the final output.

The weighted voting method assigns a certain weight to the classification results of each model according to the

TABLE 4. Comparison of four model convolution parameters.

Convolutional network	Model1	Model2	Model3	Model4
Convolutional Layer 1-5	32*1, 12, stride=[1, 1, 1, 2, 1]	32*1, 16, stride=[1, 1, 1, 2, 1]	32*1, 12, stride=[1, 1, 1, 2, 1]	16*1, 16, stride=[1, 1, 1, 2, 1]
Convolutional Layer 6-9	32*1, 24, stride=[1, 1, 2, 1]	32*1, 32, stride=[1, 1, 2, 1]	32*1, 24, stride=[1, 1, 2, 1]	16*1, 32, stride=[1, 1, 2, 1]
Convolutional Layer 10-11	32*1, 48, stride=[1, 1]	32*1, 64, stride=[1, 1]	32*1, 48, stride=[1, 1]	16*1, 64, stride=[1, 1]
Convolutional Layer 12-13	32*1, 48, stride=[2, 1]	32*1, 64, stride=[2, 1]	16*1, 48, stride=[2, 1]	16*1, 64, stride=[2, 1]
Convolutional Layer 14-17	32*1, 96, stride=[1, 1, 2, 1]	32*1, 128, stride=[1, 1, 2, 1]	16*1, 96, stride=[1, 1, 2, 1]	16*1, 128, stride=[1, 1, 2, 1]
Convolutional Layer 18-21		32*1, 256, stride=[1, 1, 2, 1]		
Convolutional Layer 21-25		32*1, 512, stride=[1, 1, 2, 1]		

The convolution parameters: convolution kernel size, number of convolution kernels, and stride length of sequence.

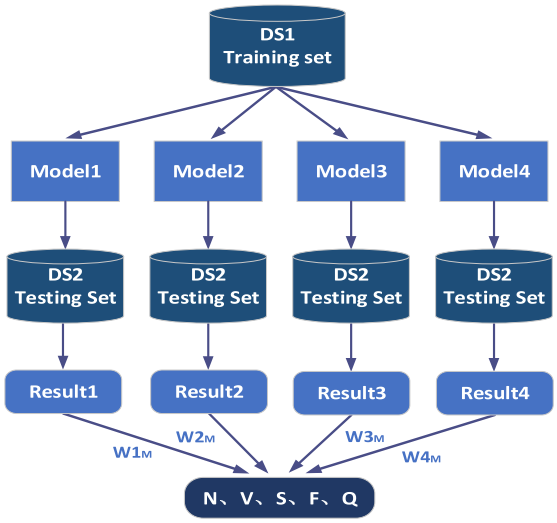

FIGURE 5. Schematic of the model integration.

classification performance of different models and finally predicts according to the majority voting method. For example, according to the classification performance of the four models for F class, Model1 has the best classification performance, Model2 is slightly inferior, and Model3 and Model4 have the worst classification performance. The F class output weights of the four models can be set as [3, 2, 1, 1]. Model1 is set as the first output priority. With the small weight of Model2, Model3, and Model4, the final result can be modified only if the classification outputs of three models are consistent.

For multi-classification problems, the effect of single classifier may be biased towards some specific categories, resulting in the lack of comprehensive comparison and analysis. The schematic of the proposed priority model integrated voting method is shown in Figure 5, and it integrates the four models to a large extent to reduce bias and achieve optimal classification effect. The DS1 set is used as the training set, and the DS2 set is used as the test set. $W1_M$, $W2_M$, $W3_M$, and $W4_M$ are the output priority representatives of the four models in M class, and the output priority is set according to the classification characteristics of each model in different categories. This method integrates the classification ability of the four models for different categories to achieve the optimal classification effect. The specific priority weight setting of four models will be given and explained in part D of Section IV.

IV. EXPERIMENTAL RESULTS

The performance of the classification model was evaluated using accuracy (Acc), sensitivity (Sen), positive predictive value (PPV), specificity (Spe), and overall accuracy (OA), which are defined as follows:

$$Acc = \frac{TN + TP}{TN + TP + FN + FP} \times 100\% \quad (5)$$

$$Sen = \frac{TP}{TP + FN} \times 100\% \quad (6)$$

$$PPV = \frac{TP}{TP + FP} \times 100\% \quad (7)$$

$$Spe = \frac{TN}{TN + FP} \times 100\% \quad (8)$$

$$OA = \frac{N_N + V_V + S_S + F_F + Q_Q}{\sum (N + V + S + F + Q)} \times 100\% \quad (9)$$

where TP, TN, FP, and FN represent true positive (TP), true negative (TN), false positive (FP), and false negative (FN) in every sample classification, respectively. N_N, V_V, S_S, F_F, and Q_Q are the number of samples predicted correctly in each category. The parameter OA is equal to the number of samples predicted correctly divided by the total number of samples.

TABLE 5. Confusion matrix and evaluation index of single- and dual-channel model with different datasets.

(A) Classification Effects of Single ECG Lead II with THML Data

		Predicted Labels					Evaluation standard				
		N	V	S	F	Q	Acc%	Sen%	PPV%	Spe%	OA%
Truth Labels	N	35570	213	309	70	5	91.40	98.35	91.37	65.83	
	V	929	5699	5	13	0	96.87	85.75	92.02	98.74	
	S	1769	218	461	0	0	94.99	18.83	59.33	99.27	90.74
	F	655	57	2	7	0	98.26	0.97	7.69	99.81	
	Q	5	6	0	1	0	99.96	0	0	99.99	

(B) Classification Effects of Dual ECG Lead with THML Data

		Predicted Labels					Evaluation standard				
		N	V	S	F	Q	Acc%	Sen%	PPV%	Spe%	OA%
Truth Labels	N	35033	93	1040	1	0	93.23	96.86	94.65	79.88	
	V	288	6334	21	2	1	98.88	95.31	96.89	99.48	
	S	1065	47	1334	2	0	95.27	54.49	55.65	97.56	92.93
	F	622	56	1	42	0	98.51	5.83	87.50	99.99	
	Q	2	7	1	1	1	99.97	8.33	50.00	99.99	

(C) Classification Effects of Dual ECG Lead with Fixed-length data

		Predicted Labels					Evaluation standard				
		N	V	S	F	Q	Acc%	Sen%	PPV%	Spe%	OA%
Truth Labels	N	9387	274	651	47	2	88.04	90.59	93.91	78.74	
	V	129	1812	56	3	0	96.27	90.60	85.63	97.29	
	S	330	16	350	0	0	92.03	50.28	33.08	94.35	87.35
	F	148	11	1	0	0	98.41	0	0	99.62	
	Q	1	3	0	0	1	99.95	20.00	33.33	99.98	

The patient records division of training set (DS1) and testing set (DS2) are according to the AAMI standard. The evaluation indexes are Acc, Sen, PPV, Spe, and OA.

Therefore, the parameter OA is used to evaluate the overall effect of the classifier.

A. INPUT CHANNEL-BASED ASSESSMENT

To compare the classification effect of single-lead ECG input and multi-lead ECG input, the following input channel-based experiment we performed. Model1 was considered as the basic model, and the THML ECG signals are input into the dual-channel model with one channel from the modified ECG lead II and the other channel from ECG lead V1. The contrast experiment is based on Model1 with single channel, and the input signals are lead II signals from the THML ECG data. The experiments used the patient data of DS1 for training and the patient data of DS2 for testing. Part (A) of Table 5 shows the confusion matrix and evaluation indexes of the single-channel models. Part (B) of Table 5 shows the confusion matrix and evaluation indexes of the dual-channel models.

Experimental results show that the dual-channel THML ECG data can improve many evaluation indexes. The positive predictive value of V class from dual ECG lead input increased from 92.02% to 96.89% compared with the single lead II input while the sensitivity increased from 85.75% to 95.31%. The positive predictive value of F class increased significantly from 7.69% to 87.50% because of the increased number of input ECG leads. The overall accuracy of the classification model also improved from 90.74% to 92.93%.

Therefore, the dual ECG lead can improve the classification effect to some extent, and the model can combine more feature information to complete the classification.

B. PRE-PROCESSING-METHOD-BASED ASSESSMENT

To compare the classification effects of different data pre-processing methods, Sets A and B were used for training by taking Model1 of dual-channel as the basic model. The THML ECG data and fixed-length ECG data, both from the DS2 set, are used for testing the models. The descriptions for Sets A and B were discussed in Section II. The results of the pre-processing method-based experiment are listed in parts (B) and (C) of Table 5. The experimental results show that classification effect of fixed-length ECG data is generally reduced compared with that of THML ECG data. The THML data performs well in the classification model, with N class and V class in particular reaching a sensitivity of more than 95%.

The THML ECG data and fixed-length ECG data have their own disadvantages and advantages. The THML ECG data relies on the accuracy of the QRS wave detection

TABLE 6. Evaluation index of four classification models.

Classification Effects for Four Models										
Evaluation standard of Model1						Evaluation standard of Model2				
Class	Acc%	Sen%	PPV%	Spe%	OA%	Class	Acc%	Sen%	PPV%	Spe%	OA%
N	93.24	96.86	94.66	79.88		N	93.04	95.57	95.59	83.76	
V	98.88	95.31	96.89	99.48		V	98.33	98.69	90.61	98.27	
S	95.27	54.49	55.65	97.56	92.93	S	95.24	52	55.71	97.68	92.5
F	98.51	5.83	87.50	99.99		F	98.45	20.39	51.76	99.7	
Q	99.97	8.33	50	99.99		Q	99.92	0	0	99.94	
Evaluation standard of Model3						Evaluation standard of Model4				
Class	Acc%	Sen%	PPV%	Spe%	OA%	Class	Acc%	Sen%	PPV%	Spe%	OA%
N	91.48	96.05	93.31	74.64		N	90.89	90.19	98.07	93.46	
V	95.83	89.72	82.83	96.86		V	93.72	96.1	70.83	93.31	
S	96.74	45.59	87.05	99.61	91.09	S	97.81	78.15	80.14	98.91	89.89
F	98.15	10.4	26.98	99.55		F	97.42	58.95	32.27	98.03	
Q	99.97	0	0	99.99		Q	99.95	0	0	99.98	

The four models are Model1, Model2, Model3, and Model4, and are designed as dual-channel input. The patient records division of training set (DS1) and testing set (DS2) are according to the AAMI standard, and each segment is THML ECG data. The evaluation indexes are Acc, Sen, PPV, Spe, and OA.

algorithm. However, the THML data can effectively improve the integrity of ECG information and improve the accuracy of the arrhythmia classification. The fixed-length ECG data has minimal restrictions on input data and strong randomness. Yet the disadvantage of fixed-length ECG is that conducting diagnosis processing for information loss is difficult and its arrhythmia recognition effect is not as good as that of the THML data.

C. FOUR CLASSIFICATION MODEL ASSESSMENT

The evaluation indexes of the four models on THML ECG data set are given in Table 6. The results show that the classification performance of Model1 is generally good. The positive predictive value of its F class is the highest, which means that the predicted error number of Model1 in class F is small, and the classification effect of other categories in Model1 has relatively good results as well. The overall accuracy of Model2 is 92.50%, second only to that of Model1. The overall accuracy of Model3 is 91.09%, but its positive predictive value for S class is 87.05%, which is higher than that of the other three models. The overall accuracy of Model4 is 89.89%, the lowest among the four models. However, the sensitivity of S class in Model4 is higher than that of the other three models, and its positive predictive value of S class is second only to that of Model3. This indicates that Model4 has learned the characteristics of S class better than the others.

D. INTEGRATED MODEL ASSESSMENT

On the basis of the above analysis, this study proposes a priority model integrated voting method combining the advantages of the above four models, which uses the majority voting and the weighted voting method discussed in Part D of Section III.

The final classification result of the integrated model adopts the priority weighted voting output according to the classification effect of each model on different categories. The priority weight of the four models is set, and $W1_M$, $W2_M$, $W3_M$, and $W4_M$ represent different output priority weight of M class in the four models. Among all the output judgments of F and Q classes, the classification results of Model1 are set to be the most weighted and output first, because these two classes have better performance in Model1 than in other models. In the output judgment of S class, the S class classification of Model3 is set as the first-level weight output, and the S class output of Model4 is set as the second-level weight output because Model3 and Model4 have better classification effects on S class, and Model3 has the best positive predictive value on S class. The remaining non-priority output categories of the four models are set as the same weight and majority voting is used to output. When the same number of votes occurs, the classification results of Model1 with the best overall accuracy will be adopted as the final output category instead of the random output because random output increases the uncertainty of the results.

The evaluation index of the integrated model are listed in Table 7. This table shows that the classification effect of the integrated model is better than that of any single model. Although it does not perform well in the identification of the Q class, the AAMI standard indicates that the classification accuracy of Q class is only for reference. On the basis of the above analysis, this study obtains the optimal classification effect by adopting the priority model integrated voting method.

TABLE 7. Confusion matrix and evaluation index of the integrated model.

Classification Effects of Integrated Model											
		Predicted Labels					Evaluation standard				
		N	V	S	F	Q	Acc%	Sen%	PPV%	Spe%	OA%
Truth Labels	N	34853	555	731	25	3	94.82	96.37	97.02	89.11	
	V	149	6446	40	11	0	98.10	96.99	90.53	98.29	
	S	420	52	1970	4	2	97.28	80.47	71.87	98.23	94.43
	F	500	57	0	164	0	98.70	22.75	80.39	99.91	
	Q	1	10	0	0	1	99.97	8.33	16.67	99.99	

The patient records division of training set (DS1) and testing set (DS2) are according to the AAMI standard, and each segment is THML data. The evaluation indexes are Acc, Sen, PPV, Spe, and OA.

V. DISCUSSION

The comparisons with previous arrhythmia classification methods [27], [28], [36]–[41] are presented in Table 8. All of studies considered used the MIT-BIH arrhythmia database as sample data and classified arrhythmia according to AAMI standards. The AAMI standard points out that the classification accuracy of Q class is for reference only, which is why most studies have not analyzed the Q class at present. Therefore, Q class is not compared in this part.

The results of the inter-patient experiment were persuasive due to the unified standard. The input data formats and the classifiers used in each study are listed in Table 8. Kandala *et al.* [27] has achieved the sensitivity of N class and V class exceeding 95%, but the small number of categories do a poor job of classification. Shi *et al.* [28] studied on XGBoost to reduce the impact of imbalance in the dataset, and improved the sensitivity of S class to 91.7%. Zhou *et al.* [35] used Long-short-term memory network to classify S class to positive predictive values of S and F class. Wang *et al.* [36] have better performance in N and S class, in which sensitivities are more than 90%. Essa *et al.* [37] and Liu *et al.* [38] focused on the small number arrhythmia categories, and had breakthroughs in the F and S classes, respectively. Han *et al.* [39] took advantage of raw ECG records of variable length, and the sensitivity of N class, V class, and S class exceeded 90%. Wang *et al.* [40] achieved high indicators, including positive predictive value of N and V class reached 93%, and the positive predictive value of S class was 89.5%. Therefore, most studies use lead II ECG and fixed-length cutting method to preprocess data samples, while ignoring the integrity of ECG signals and the timing characteristic of physiological signals. The proposed method uses the strong parallelism and adaptability of neural network to classify ECG signals, and the ensemble learning method can also be used for error analysis and performance integration of multi-classification problems. Moreover, the research has excellent recognition ability for N class, but the recognition effect for V, S and F class is uneven. However, in clinical application, ECG recognition of abnormal categories is of great significance to heart disease.

Table 8 shows that the overall accuracy of the proposed method is 94.4%, which is among the highest in recent research. Compared with other studies, the accuracy of its N class is not outstanding. For the relatively small number of V, S, and F classes, the positive predictive values are 90.5%, 71.9%, and 80.4%, respectively. The performance effect of the rare category is improved, and their positive predictive values are higher than those in most related studies. Although the training set is expanded by means of data balancing, there are still low indexes of S and F classes, mainly due to the following two reasons. On the one hand, models have difficulty learning the characteristics of the small number of categories, because the number of N class is far greater than the number of other classes. On the other hand, there were only a few patients' samples of S and F classes in the MIT-BIH arrhythmia database and no new data samples were introduced into the data balance therefore resulting in insufficient sample specificity in the training process of the proposed network. Although the study of the N category is comprehensive, the study of rare categories is more helpful to promote the development of ECG recognition and diagnosis.

This study used THML ECG data and data balancing to alleviate the shortage problem in ECG samples and achieve a certain effect. Through a series of ablation experiments, the superiority and feasibility of THML data, 1D-CNN architecture, and the proposed integrated method were proven. Despite the proposed method achieving better performance, it has several aspects that can be improved:

1) The above analysis shows that the THML data can effectively improve the integrity of ECG information and improve the accuracy of the arrhythmia classification well. However, the pre-processing method of THML ECG data relies on the accuracy of the QRS wave detection algorithm. If the THML data is used in clinical identification and diagnosis, then the QRS wave detection algorithm needs to be improved.

TABLE 8. Comparison of ECG arrhythmia classification effect between the raised method and previous works.

Methods	Input Segment Format	the lead of ECG	Classifier	Acc%	N		V		S		F	
					Sen%	PPV%	Sen%	PPV%	Sen%	PPV%	Sen%	PPV%
Kandala [27] (2019)	300 sampling points/ each segment	Lead II	Nonlinear Morphological Features and Voting Method	-	94.1	95.4	99.7	90.3	42.4	7.9	89.2	10.7
Shi [28] (2019)	Single heartbeat/ each segment	Lead II	XGBoost Hierarchical Classification Method	92.1	92.1	99.5	95.1	88.1	91.7	46.2	61.6	15.2
Zhou [35] (2019)	900 sampling points/ each segment	Lead II	Long-short-term memory network	-	97.2	98.55	95.78	75.15	87.07	90.08	19.59	40.86
Wang [36] (2020)	Single heartbeat/ each segment	Lead II	Dual Fully CNN	93.4	95.1	98.3	84.1	89.5	90.3	43.5	-	-
Essa [37] (2020)	180 sampling points/ each segment	Lead II	Multi-model Deep Learning Ensemble	-	-	-	93.91	94.55	65.51	66.19	19.33	41.67
Liu [38] (2020)	556 ms/ each segment	Lead II	High Order Spectrum and 2D Graph Fourier Transform	-	-	-	52.7	90.1	36.1	87.9	-	-
Han [39] (2021)	Variable Length/ each segment	Lead II	Multi-scale Convolution Structure	-	95	99.7	92.7	95.7	91.3	42	-	-
Wang [40] (2021)	200 sampling points/ each segment	Lead II	Continuous Wavelet Transform and CNN	-	99.4	98.2	95.7	93.3	74.6	89.5	0.3	2
Proposed method	Three-heartbeat/ each segment	Lead II and lead V1	1D-CNN with Multi-Channel and Priority Model Integrated Voting Method	94.4	96.4	97	97	90.5	80.5	71.9	22.8	80.4

2) In recent studies, an increasing number of hybrid deep learning models are applied in biological signal analysis. We can find more suitable deep learning methods for the THML ECG signal to improve the performance and hence the classification accuracy of the model. For example, CNN can be combined with the long short-term memory model to detect arrhythmia signals. Furthermore, time sequence information of ECG signal can be considered to improve the classification effect of the model.
3) The multi-heartbeat segment ECG identification method in this study is currently used for multi-category classification of a single label, but multiple cardiac diseases still occur simultaneously in clinical practice. Therefore, further study on the multi-label classification model is needed to provide a basis for future ECG intelligent interpretation.
4) The lack of ECG data samples is an important factor limiting the development of ECG recognition. The data samples can be expanded by the following two schemes: one is to introduce new patient records to meet the characteristics of independent and same distribution; the other is to mine existing data, such as the joint use of multi-lead ECG to strengthen the analysis and research of other lead data.

VI. CONCLUSION

The study innovatively proposed a THML ECG recognition method for arrhythmia classification based on the dual-channel one-dimensional convolutional neural network (1D-CNN) model and the priority model integrated voting method. Under the inter-patient experiments, the results show that the overall average accuracy of the integrated model is 94.4%. The sensitivity of N, V, S, and F classes is 96.4%,

97.0%, 80.5%, and 22.75%, respectively, and their positive predictive value of N, V, S, and F classes is 97.0%, 90.5%, 71.9%, and 80.4%, respectively. Compared with the existing literature, this method can improve the classification accuracy in arrhythmia categories, proving the practicability and theoretical feasibility of the THML ECG signal that contains the important spatial and temporal characteristics of ECG signal. Moreover, this study strengthened the adaptability of 1D-CNN architecture to THML ECG sequence data and provided a solution for learning result integration of multi-classification neural networks by using priority model integrated voting method. The proposed design of the data pre-processing scheme, arrhythmia classifier and training verification method matching the THML ECG data contributes to the intelligent recognition research of arrhythmia disease in electrocardiology.

ACKNOWLEDGMENT

The authors are grateful to the Fujian Integrated Circuit Design Center, College of Physics and Information Engineering, Fuzhou University, for providing their research laboratory, EDA tools, electronic components, and measuring instruments.

REFERENCES

[1] L.-H. Wang, W.-Z. Dong, J.-Z. Chen, F.-X. Wang, and M.-H. Fan, "Low-power low-data-loss bio-signal acquisition system for intelligent electrocardiogram detection," *IEICE Electron. Exp.*, vol. 14, no. 4, 2017, Art. no. 20161142, doi: 10.1587/elex.14.20161142.

[2] B. K. Kennedy and S. L. Berger, "Geroscience: Linking aging to chronic disease," *Cell*, vol. 159, no. 4, pp. 709–713, Nov. 2014, doi: 10.1016/j.cell.2014.10.039.

[3] L.-H. Wang, T.-Y. Chen, K.-H. Lin, Q. Fang, and S.-Y. Lee, "Implementation of a wireless ECG acquisition SoC for IEEE 802.15.4 (ZigBee) applications," *IEEE J. Biomed. Health Informat.*, vol. 19, no. 1, pp. 247–255, Jan. 2015, doi: 10.1109/JBHI.2014.2311232.

[4] E. G. Lakatta and D. Levy, "Arterial and cardiac aging: Major shareholders in cardiovascular disease enterprises: Part I: Aging arteries: A 'set up' for vascular disease," *Circulation*, vol. 107, no. 1, pp. 139–146, Jan. 2003, doi: 10.1161/01.CIR.0000048892.83521.58.

[5] R. Lozano and M. Naghavi, "Global and regional mortality from 235 causes of death for 20 age groups in 1990 and 2010: A systematic analysis for the global burden of disease study 2010," *Lancet*, vol. 381, p. 628, Feb. 2013, doi: 10.1016/S0140-6736(13)60346-3.

[6] G. A. Roth, M. H. Forouzanfar, A. E. Moran, R. Barber, G. Nguyen, V. L. Feigin, M. Naghavi, G. A. Mensah, and C. J. L. Murray, "Demographic and epidemiologic drivers of global cardiovascular mortality," *New England J. Med.*, vol. 372, no. 14, pp. 1333–1341, Apr. 2015, doi: 10.1056/NEJMoa1406656.

[7] M. Llamedo and J. P. Martinez, "Heartbeat classification using feature selection driven by database generalization criteria," *IEEE Trans. Biomed. Eng.*, vol. 58, no. 3, pp. 616–625, Mar. 2011, doi: 10.1109/TBME.2010.2068048.

[8] Z. Zhang, J. Dong, X. Luo, K.-S. Choi, and X. Wu, "Heartbeat classification using disease-specific feature selection," *Comput. Biol. Med.*, vol. 46, pp. 79–89, Mar. 2014, doi: 10.1016/j.compbiomed.2013.11.019.

[9] T. Mar, S. Zaunseder, J. P. Martínez, M. Llamedo, and R. Poll, "Optimization of ECG classification by means of feature selection," *IEEE Trans. Biomed. Eng.*, vol. 58, no. 8, pp. 2168–2177, Aug. 2011, doi: 10.1109/TBME.2011.2113395.

[10] S. Kiranyaz, T. Ince, J. Pulkkinen, and M. Gabbouj, "Personalized long-term ECG classification: A systematic approach," *Expert Syst. Appl.*, vol. 38, no. 4, pp. 3220–3226, Apr. 2011, doi: 10.1016/j.eswa.2010.09.010.

[11] P. Li, Y. Wang, J. He, L. Wang, Y. Tian, T.-S. Zhou, T. Li, and J.-S. Li, "High-performance personalized heartbeat classification model for long-term ECG signal," *IEEE Trans. Biomed. Eng.*, vol. 64, no. 1, pp. 78–86, Jan. 2017, doi: 10.1109/TBME.2016.2539421.

[12] C. C. Lin and C. M. Yang, "Heartbeat classification using normalized RR intervals and wavelet features," in *Proc. Int. Symp. Comput., Consum. Control*, Jun. 2014, pp. 650–653, doi: 10.1109/IS3C.2014.175.

[13] C. Ye, B. V. K. V. Kumar, and M. T. Coimbra, "Heartbeat classification using morphological and dynamic features of ECG signals," *IEEE Trans. Biomed. Eng.*, vol. 59, no. 10, pp. 2930–2941, Oct. 2012, doi: 10.1109/TBME.2012.2213253.

[14] L.-H. Wang, W. Zhang, M.-H. Guan, S.-Y. Jiang, M.-H. Fan, P. A. R. Abu, C.-A. Chen, and S.-L. Chen, "A low-power high-data-transmission multi-lead ECG acquisition sensor system," *Sensors*, vol. 19, no. 22, p. 4996, Nov. 2019, doi: 10.3390/s19224996.

[15] T. Zhuang, C. Feng, L.-H. Wang, J. Gao, and Y. Yang, "Hardware implementation of real-time ECG R-wave detection with wavelet transform algorithm," in *Proc. 4th Int. Conf. Commun. Inf. Process. (ICCIP)*, Qingdao, China, 2018, pp. 305–308.

[16] S.-Y. Jiang and L.-H. Wang, "Enhanced machine learning feature selection algorithm for cardiac arrhythmia in a personal healthcare application," in *Proc. IEEE Asia Pacific Conf. Postgraduate Res. Microelectron. Electron. (PrimeAsia)*, Chengdu, China, Oct. 2018, pp. 39–42.

[17] X. Tang, Z. Ma, Q. Hu, and W. Tang, "A real-time arrhythmia heartbeats classification algorithm using parallel delta modulations and rotated linear-kernel support vector machines," *IEEE Trans. Biomed. Eng.*, vol. 67, no. 4, pp. 978–986, Apr. 2020, doi: 10.1109/TBME.2019.2926104.

[18] U. R. Acharya, H. Fujita, M. Adam, O. S. Lih, T. J. Hong, V. K. Sudarshan, and J. E. Koh, "Automated characterization of arrhythmias using nonlinear features from tachycardia ECG beats," in *Proc. IEEE Int. Conf. Syst., Man, Cybern. (SMC)*, Budapest, Hungary, Oct. 2016, pp. 533–537, doi: 10.1109/SMC.2016.7844294.

[19] T. Ince, S. Kiranyaz, and M. Gabbouj, "A generic and robust system for automated patient-specific classification of ECG signals," *IEEE Trans. Biomed. Eng.*, vol. 56, no. 5, pp. 1415–1426, May 2009, doi: 10.1109/TBME.2009.2013934.

[20] J. Rodriguez, A. Goni, and A. Illarramendi, "Real-time classification of ECGs on a PDA," *IEEE Trans. Inf. Technol. Biomed.*, vol. 9, no. 1, pp. 23–34, Mar. 2005, doi: 10.1109/TITB.2004.838369.

[21] L. S. C. de Oliveira, R. V. Andreao, and M. Sarcinelli-Filho, "Premature ventricular beat classification using a dynamic Bayesian network," in *Proc. Annu. Int. Conf. IEEE Eng. Med. Biol. Soc.*, Boston, MA, USA, Aug. 2011, pp. 4984–4987.

[22] A. K. Sharma, S. Chaurasia, and D. K. Srivastava, "Sentimental short sentences classification by using CNN deep learning model with fine tuned Word2Vec," *Proc. Comput. Sci.*, vol. 167, pp. 1139–1147, Sep. 2020, doi: 10.1016/j.procs.2020.03.416.

[23] S. Shimazaki, H. Kawanaka, H. Ishikawa, K. Inoue, and K. Oguri, "Cuffless blood pressure estimation from only the waveform of photoplethysmography using CNN," in *Proc. 41st Annu. Int. Conf. IEEE Eng. Med. Biol. Soc. (EMBC)*, Berlin, Germany, Jul. 2019, pp. 5042–5045.

[24] G. S. P. Mok, Q. Zhang, J. Sun, D. Zhang, P. H. Pretorius, and M. A. King, "Preliminary investigation of auto-classification of respiratory trace using convolutional neural network for adaptive respiratory gated myocardial perfusion SPECT," in *Proc. IEEE Nucl. Sci. Symp. Med. Imag. Conf. (NSS/MIC)*, Manchester, U.K., Oct. 2019, pp. 1–3.

[25] J. Brieva, H. Ponce, and E. Moya-Albor, "A contactless respiratory rate estimation method using a Hermite magnification technique and convolutional neural networks," *Appl. Sci.*, vol. 10, no. 2, p. 607, Jan. 2020, doi: 10.3390/app10020607.

[26] Y. Zhao, J. Cheng, and P. Zhang, "ECG classification using deep CNN improved by wavelet transform," *Comput., Mater. Continua*, vol. 64, no. 3, pp. 1615–1628, Jan. 2020, doi: 10.32604/cmc.2020.09938.

[27] R. N. Kandala, R. Dhuli, P. Pławiak, G. R. Naik, H. Moeinzadeh, G. D. Gargiulo, and S. Gunnam, "Towards real-time heartbeat classification: Evaluation of nonlinear morphological features and voting method," *Sensors*, vol. 19, no. 23, p. 5079, Nov. 2019, doi: 10.3390/s19235079.

[28] H. Shi, H. Wang, Y. Huang, L. Zhao, C. Qin, and C. Liu, "A hierarchical method based on weighted extreme gradient boosting in ECG heartbeat classification," *Comput. Methods Programs Biomed.*, vol. 171, pp. 1–10, Apr. 2019, doi: 10.1016/j.cmpb.2019.02.005.

[29] X. Yang, X. Zhang, M. Yang, and L. Zhang, "12-lead ECG arrhythmia classification using cascaded convolutional neural network and expert feature," *J. Electrocardiol.*, vol. 67, pp. 56–62, Jul. 2021, doi: 10.1016/j.jelectrocard.2021.04.016.

[30] P. Jain, P. Gajbhiye, R. K. Tripathy, and U. R. Acharya, "A two-stage deep CNN architecture for the classification of low-risk and high-risk hypertension classes using multi-lead ECG signals," *Informat. Med. Unlocked*, vol. 21, 2020, Art. no. 100479, doi: 10.1016/j.imu.2020.100479.
[31] U. R. Acharya, H. Fujita, S. L. Oh, Y. Hagiwara, J. H. Tan, and M. Adam, "Automated detection of arrhythmias using different intervals of tachycardia ECG segments with convolutional neural network," *Inf. Sci.*, vol. 405, no. 1, pp. 81–90, Sep. 2017, doi: 10.1016/j.ins.2017.04.012.
[32] *Testing and Reporting Performance Results of Cardiac Rhythm and ST Segment Measurement Algorithms*, ANSI/AAMI Standard EC57, 2012.
[33] P. de Chazal and R. B. Reilly, "A patient-adapting heartbeat classifier using ECG morphology and heartbeat interval features," *IEEE Trans. Biomed. Eng.*, vol. 53, no. 12, pp. 2535–2543, Dec. 2006, doi: 10.1109/TBME.2006.883802.
[34] H. M. Haqqani and F. E. Marchlinski, "The surface electrocardiograph in ventricular arrhythmias: Lessons in localisation," *Heart, Lung Circulat.*, vol. 28, no. 1, pp. 39–48, Jan. 2019, doi: 10.1016/j.hlc.2018.08.025.
[35] R. Zhou, X. Li, B. Yong, Z. Shen, C. Wang, Q. Zhou, Y. Cao, and K. C. Li, "Arrhythmia recognition and classification through deep learning-based approach," *Int. J. Comput. Sci. Eng.*, vol. 19, no. 4, p. 506, 2019, doi: 10.1504/ijcse.2019.101897.
[36] H. Wang, H. Shi, K. Lin, C. Qin, L. Zhao, Y. Huang, and C. Liu, "A high-precision arrhythmia classification method based on dual fully connected neural network," *Biomed. Signal Process. Control*, vol. 58, Apr. 2020, Art. no. 101874, doi: 10.1016/j.bspc.2020.101874.
[37] E. Essa and X. Xie, "An ensemble of deep learning-based multi-model for ECG heartbeats arrhythmia classification," *IEEE Access*, vol. 9, pp. 103452–103464, 2021, doi: 10.1109/access.2021.3098986.
[38] S. Liu, J. Shao, T. Kong, and R. Malekian, "ECG arrhythmia classification using high order spectrum and 2D graph Fourier transform," *Appl. Sci.*, vol. 10, no. 14, p. 4741, Jul. 2020, doi: 10.3390/app10144741.
[39] C. Han, F. Yu, P. Wang, R. Huang, X. Huang, and L. Cui, "Length, no longer matters: A real length adaptive arrhythmia classification model with multi-scale convolution," in *Proc. IEEE Int. Conf. Acoust., Speech Signal Process. (ICASSP)*, New York, NY, USA, Jun. 2021, pp. 1295–1299, doi: 10.1109/ICASSP39728.2021.9414616.
[40] T. Wang, C. Lu, Y. Sun, M. Yang, C. Liu, and C. Ou, "Automatic ECG classification using continuous wavelet transform and convolutional neural network," *Entropy*, vol. 23, no. 1, p. 119, Jan. 2021, doi: 10.3390/e23010119.

LIANG-HUNG WANG (Senior Member, IEEE) was born in Tainan, Taiwan, in 1976. He received the B.S. and M.S. degrees in electrical engineering from I-Shou University, Kaohsiung, Taiwan, in 2000 and 2003, respectively, and the Ph.D. degree from the Institute of Electrical Engineering, National Chung Cheng University, Chiayi, Taiwan, in 2013. He joined Fuzhou University, China, in 2014, where he is currently a Professor with the Department of Microelectronics. His current research interests include the low-power wireless ECG signal acquisition ICs design, automatic identification and classification of ECG images features, and cardiac medical information analysis with artificial intelligence computer vision processing. He is a member of the IEEE Circuits and Systems Society, the IEEE Solid-State Circuits Society, the IEEE Consumer Electronics Society, and the IEEE Engineering in Medicine and Biology Society. He served as the Publicity Chair and the Publication Chair for the IEEE 2014 and 2015 International Symposium on Bioelectronics and Bioinformatics and a Technical Program Chair Member for the 2015 IEEE International Conference on Biomedical and Health Informatics, and the Publication Chair and the Publicity Chair for the IEEE ICCP/HSIC2016, IEEE ICCE-TW2017, and IEEE ISNE2018. Since 2013, he has been serving as the Educational Affairs Chair for the IEEE Solid-State Circuits Society Tainan Chapter.

YAN-TING YU was born in Fuqing, Fujian, China, in 1998. She received the B.S. degree from the College of Physics and Information Engineering, Fuzhou University, Fujian, in July 2020. She is currently pursuing the degree with Fuzhou University. Her research interests include ECG signal processing, arrhythmia classification, and deep learning.

WEI LIU was born in Bijie, Guizhou, in 1996. She received the B.S. degree from the College of Physics and Information Engineering, Fuzhou University, Fujian, China, in July 2019. She is currently pursuing the degree with Fuzhou University. Her research interests include monitoring of blood pressure, machine learning, and transfer learning.

LU XU was born in Jian, Jiangxi, in 1995. She received the B.S. degree in communication engineering from Yantai University, Shandong, China, in July 2017. She was graduated at Fuzhou University, in 2020. Her research interests include deep learning and arrhythmia classification.

CHAO-XIN XIE was born in Nanping, Fujian, in 1998. He received the B.S. degree from the College of Physics and Information Engineering, Fuzhou University, Fujian, China, in July 2020. He is currently pursuing the degree with Fuzhou University. His research interests include mobile health, machine learning, and arrhythmia classification.

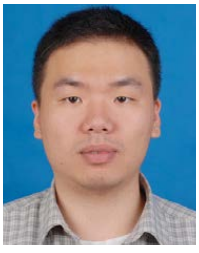

TAO YANG received the bachelor's degree in physics and the Ph.D. degree in microelectronics and solid-state electronics from Xiamen University, in 2005 and 2012, respectively. He joined the Department of Microelectronics, College of Physics and Information Engineering, Fuzhou University, and engaged in teaching and scientific research. He is currently a member of the FJICC-CBIC Team. His research interests include embedded systems, analog circuit front-end design, and machine learning algorithm for biological signal analysis.

I-CHUN KUO was born in Kaohsiung, Taiwan, in 1981. She received the B.S. and M.S. degrees from the College of Applied Sciences Management and Administration, Tainan University, Tainan, Taiwan, in 2010 and 2013, respectively. She joined Fuzhou University, China, in 2020, where she is currently a Lecturer with the College of Biological Science and Engineering. Her research interests include data analysis of bioinformation and biosignal.

XIN-KANG WANG was born in Longyan, Fujian, in 1972. He received the B.S. degree from Qingdao University, in 1996, and the M.S. degree from Fujian Medical University, China, in 2007. He is currently the Director of cardiovascular medicine and leads the ECG Diagnosis Department, Fujian Provincial Hospital and Fujian Provincial Hospital South Branch, Fujian, China. His research interests include cardiovascular medicine, cardiac electrophysiology, and intelligence medical. He served as a member for the Medical Professional Standing Committee in the China Health Information and Big Data Association, the China Electrocardiology Technology Branch, the China Rehabilitation Technology and Development Association, and the China Medical Health International Exchange Association Rhythm and Electrocardiology Branch. He is the Vice Chairperson of China ECG Alliance.

JIE GAO was born in Fuzhou, Fujian, in 1987. She graduated from Fujian Medical University, China, in 2011, with major in clinical medicine. She is currently pursuing the master's degree in clinical medicine with Fujian Medical University. She is also working with the ECG Diagnosis Department, Fujian Provincial Hospital. Her research interests include cardiac electrophysiology and esophageal electrophysiology. She won the Second Prize in the National Clinical Electrocardiogram Competition in 2017.

PAO-CHENG HUANG was born in Tainan, Taiwan, in 1976. He received the M.S. degree from the Department of Computer Science and Information Engineering, Leader University, Tainan, in 2005, and the Ph.D. degree from the Department of Electrical Engineering, National Chen Kung University, Tainan, in 2016. He joined Fujian Agriculture and Forestry University, Fujian, China, in 2016, where he is currently a Lecturer with the College of Computer and Information Sciences. His current research interests include fluid delivery systems and biomedical electronic applications.

SHIH-LUN CHEN (Member, IEEE) received the B.S., M.S., and Ph.D. degrees in electrical engineering from the National Cheng Kung University, Tainan, Taiwan, in 2002, 2004, and 2011, respectively. He was an Assistant Professor with the Department of Electronic Engineering, Chung Yuan Christian University, Taiwan, from 2011 to 2014, an Associate Professor with the Department of Electronic Engineering, Chung Yuan Christian University, from 2014 to 2017, where he has been a Professor with the Department of Electronic Engineering, since 2017. His current research interests include VLSI chip design, image processing, wireless body sensor networks, the Internet of Things, wearable devices, data compression, fuzzy logic control, bio-medical signal processing, and reconfigurable architecture. He was a recipient of the Outstanding Teaching Award from Chung Yuan Christian University in 2014 and 2019, respectively.

WEI-YUAN CHIANG received the B.S. degree in physics from Chung Yuan Christian University, Taoyuan, Taiwan, in 2001, and the M.S. and Ph.D. degrees in physics from the National Tsing Hua University, Hsinchu, Taiwan, in 2003 and 2008, respectively. He was an Assistant Professor with the Department of Electrical Engineering, Ming Chi University of Technology, Taiwan, from 2015 to 2020, and an Assistant Engineer with the Light Source Division, National Synchrotron Radiation Research Center, since 2021. His current research interests include electromagnetism, microwave source, microwave processing of advanced material, and microwave physics and engineering.

PATRICIA ANGELA R. ABU (Member, IEEE) received the B.S. degree in electronics and communications engineering from Ateneo de Manila University, Philippines, in 2007, the M.S. degree in electronics engineering major in microelectronics from Chung Yuan Christian University, Chung-Li, Taiwan, in 2009, and the Ph.D. degree in computer science from Ateneo de Manila University, in 2012. She is currently the Research Laboratory Head of the Ateneo Laboratory for Intelligent Visual Environment (ALIVE) and an Assistant Professor at the Department of Information Systems and Computer Science (DISCS), Ateneo de Manila University. Her current research interests include image processing and computer vision with applications that revolve on biomedical and transportation/traffic, anomaly detection, and the IoT systems which granted ALIVE several best research paper and presentation awards both here and abroad.